A composite theory and its potential with respect to materials design

Nielsen, Lauge Fuglsang

Publication date:
2007

Document Version
Publisher's PDF, also known as Version of record

BYG DTU

A composite theory and its potential with respect to materials design

Lauge Fuglsang Nielsen

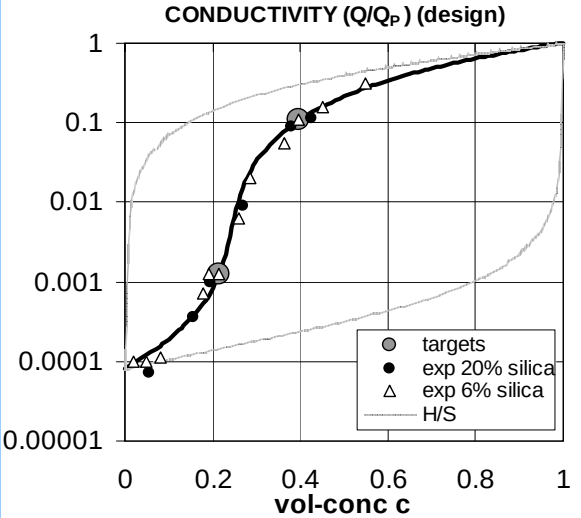

Conductivity in composite designed from prescribed chloride diffusitivity at two concentrations (gray dots).

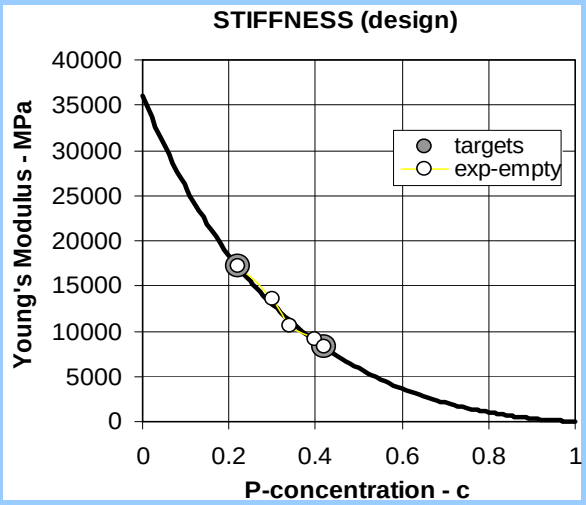

Stiffness of porous material designed from stiffness at two porosities (gray dots).

DANMARKS
TEKNISKE
UNIVERSITET

BYG•DTU R-150
ISSN 1601-2917
ISBN 87-7877-222-2

A composite theory and its potential with respect to materials design

Lauge Fuglsang Nielsen*)

Abstract: An operational summary of a composite theory previously developed by the author is presented in this paper. 'Global' property solutions are presented which are valid for any composite geometry. Properties looked at are mechanical, such as stiffness, eigenstrain/stress (e.g. shrinkage and thermal expansion), and physical, such as various conductivities with respect to heat, electricity, and diffusion.

'Local' property solutions applying for specific composites are obtained from the global solutions introducing geometry specific, so-called shape functions. Examples are presented, demonstrating a very satisfying agreement between material properties determined experimentally and such properties predicted by the theory considered.

Further support for the author's theory can be found in his original work: The geometrical concept applied includes simple geometrical models (such as spheres, layers, and fibers) on which well-known composite theories from the literature are based. This means that composite properties predicted by the author's theory coincide with such predicted by authors such as Hashin, Budiansky, Böttcher, and Maxwell.

In a special section of the paper the theory is examined with respect to its potential with respect to materials design. Examples are presented, demonstrating how the prediction method can be inversed to determine types of composite geometry from prescribed composite properties, such as Young's moduli and conductivities.

A software ('COMPREDES') is prepared with application programs covering both the prediction aspects and the design aspects of the method presented. On request this software is available for the reader who has a special interest in the subjects considered.

Some ideas for further research in the prediction and design areas considered are suggested at the end of the paper.

Content

*) Dep. Civ. Eng., Tech. Uni. Denmark, dk-2800 Lyngby, Denmark - e-mail: lfn@byg.dtu.dk

A composite theory and its potential with respect to materials design

Lauge Fuglsang Nielsen*)

1. INTRODUCTION

The present paper is based on a composite theory for isotropic composite materials presented by the author in (1,2) by whom 'global' solutions to composite problems can be determined for any composite, irrespective of geometry. 'Local' solutions applying for composites with specific geometries are subsequently obtained from the global solutions introducing so-called shape functions.

In the author's original work (1,2) is shown that the theory is consistent with any well-known composite theory presented in the literature, such as in Hashin, Budiansky, Böttcher, and Maxwell (3,4,5,6).

The 'global' feature of the theory means that it has a potential with respect to materials design. In order to study this potential more closely, an operational summary of the author's composite theory (1) is presented in the first part of this paper. Some preliminary studies on materials design are then made in the second part of the paper.

Some ideas for further research in the areas considered on prediction and design are suggested at the end of the paper

Remark: It is not the purpose of the present paper to consider viscoelastic composites. Readers especially interested in such materials are referred to (1,2) where the results presented in this paper are generalized to include viscoelastic composites.

1.1 General conditions

The composites considered are isotropic mixtures of two components: phase P and phase S. The amount of phase P in phase S is quantified by the so-called volume concentration defined by $c = V_P/(V_P+V_S)$ where volumes are denoted by V. It is assumed that both phases exhibit linearity between response and gradient of potentials, which they are subjected to. For example: Mechanical stress versus deformation (Hooke's law), heat flow versus temperature, flow of electricity versus electric potential, and diffusion of a substance versus concentration of substance.

In general, flexible phase geometries are considered which can adjust them selves to form a tight composite. The adjustment can be natural (as in concretes), or organic (as in bone structures), or it can be the result of a melting processing, or compaction (as in sintered powder composites).

The composite properties specifically considered are stiffness, eigenstrain, and various conductivities as related to volume concentration, composite geometry, and phase properties such as Young's moduli E_P and E_S (with stiffness ratio $n = E_P/E_S$), eigenstrains λ_P and λ_S, and conductivities Q_P and Q_S (with conductivity ratio $n_Q = Q_P/Q_S$). Further notations used in the text are explained in the list of notations at the end of the paper.

In general the following assumptions are introduced:

---

*) Dep. Civ. Eng., Tech. Uni. Denmark, dk-2800 Lyngby, Denmark - e-mail: lfn@byg.dtu.dk

- For simplicity (but also to reflect most composite problems encountered in practice) stiffness and stress results presented assume an elastic phase behavior with Poisson's ratios $\nu = 0.2$ (in practice $\nu \approx 0.2$). This means that, whenever stiffness and stress expressions are presented, they can be considered as generalized quantities, applying for any loading mode: shear, volumetric, as well as uni-axial. For example, E/E_S can also be used to predict the composite shear modulus, G/G_S, and the composite bulk modulus, K/K_S, normalized with respect to the phase S properties. In a similar way the phase stresses[1)], σ_P/σ and σ_S/σ, also apply independently of loading mode as long as both phase stress modes (σ_P,σ_S) and composite (external) stress modes (σ) are the same.

- Not to exaggerate our present knowledge of composite geometries it has, deliberately, been chosen to keep geometry described by simple mathematical expressions.

Formally, the original theory in (1,2) is simplified very much by these assumptions: Only the volumetric analysis, for example, has to be considered - and the tensor notation can be dropped.

1.2 Global composite properties

As previously mentioned, the theory in (1,2) predicts global solutions for composite problems. Examples are presented in Equations 1 - 5 with symbols explained in the list of notations at the end of this paper. The influence of geometry on these solutions is 'hidden' in the so-called geo-functions, θ, illustrated in Figure 1.

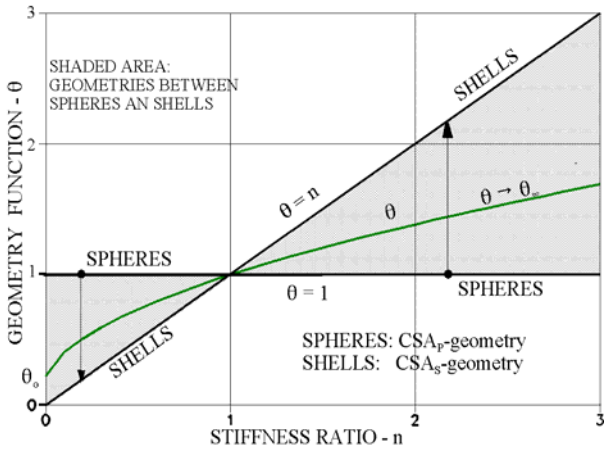

Figure 1. *The overall influence of phase P geometry on the geo-function θ for stiffness. Phase P being spheres in a continuous phase S (CSA_P) is defined by $\theta \equiv 1$. Phase S being spheres in a continuous phase P (CSA_S) is defined by $\theta \equiv n$. Composites with geometries between these extremes have θ in shaded area.*
For the geo-function θ_Q for conductivity: Replace the n-axis with an n_Q axis and θ with θ_Q. The shaded area is bounded by $\theta_Q \equiv 2$ (for CSA_P) and $\theta_Q \equiv 2n_Q$ (for CSA_S).

Stiffness :

$$e = \frac{E}{E_S} = \frac{n + \theta[1 + c(n - 1)]}{n + \theta - c(n - 1)} \qquad (1)$$

Stress due to external load (σ)

$$\frac{\sigma_P}{\sigma} = \frac{n(1 + \theta)}{n + \theta[1 + c(n - 1)]} \quad ; \quad \frac{\sigma_S}{\sigma} = \frac{n + \theta}{n + \theta[1 + c(n - 1)]} \qquad (2)$$

Eigenstrain (linear)

$$\lambda = \lambda_S + \Delta\lambda \frac{1/e - 1}{1/n - 1} \quad ; \quad (\Delta\lambda = \lambda_P - \lambda_S) \qquad (3)$$

1) As in (1,2), phase stress and phase strain are defined in this paper by their respective volume averages in phase considered.

Eigenstress (hydrostatic)

$$p_P = -\frac{5}{3} E_S \Delta\lambda \frac{c(1/n - 1) - (1/e - 1)}{c(1/n - 1)^2} \quad ; \quad p_S = -\frac{c}{1 - c} p_P \qquad (4)$$

Conductivity :

$$q = \frac{Q}{Q_S} = \frac{n_Q + \theta_Q [1 + c(n_Q - 1)]}{n_Q + \theta_Q - c(n_Q - 1)} \qquad (5)$$

1.2.1 Bounds on stiffness and conductivity

The above stiffness- and conductivity predictions are bounded as follows between the exact solutions for the CSA composites illustrated in Figures 2 and 3.

The former bounds are obtained from Equation 1 introducing $\theta \equiv 1$ and $\theta \equiv n$ respectively. The latter bounds are obtained from Equation 5 introducing $\theta_Q \equiv 2$ and $\theta_Q \equiv 2n_Q$ respectively. The bounds such determined are the same as can be obtained from the studies made by Hashin and Shtrikman in (7) on composite stiffness and in (8) on composite conductivity. The bounds are subsequently referred to by H/S.

Stiffness-bounds

$$\frac{n + 1 + c(n - 1)}{n + 1 - c(n - 1)} \le e = \frac{E}{E_S} < n \frac{2 + c(n - 1)}{2n - c(n - 1)}$$

valid for $n > 1$; reverse signs when $n < 1$

(6)

Conductivity-bounds

$$\frac{n_Q + 2[1 + c(n_Q - 1)]}{n_Q + 2 - c(n_Q - 1)} \le q = \frac{Q}{Q_S} < n_Q \frac{3 + 2c(n_Q - 1)}{3n_Q - c(n_Q - 1)}$$

valid for $n_Q > 1$; reverse signs when $n_Q < 1$

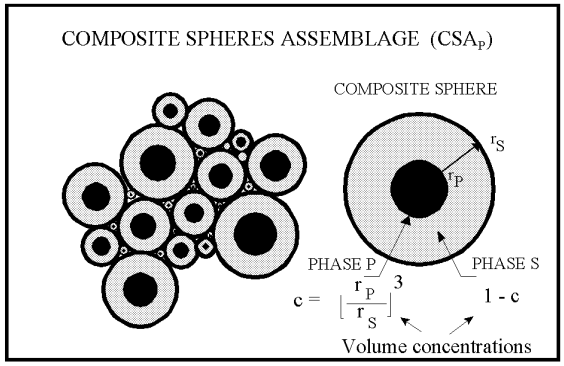

Figure 2. *Composite Spheres Assemblage with phase P particles, CSA$_P$.*

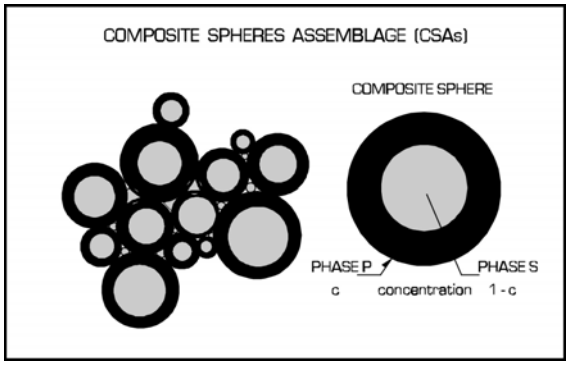

Figure 3. *Composite Spheres Assemblage with phase S particles, CSA$_S$.*

2. SPECIFIC COMPOSITES

2.1 Geometry – an overview

Geometries in a composite changes as the result of volume transformations associated with increasing phase P concentration. We will think of changes as they are stylized in Figure 4: At increasing concentration, from c = 0, discrete phase P elements agglomerate and change their shapes approaching a state at the so-called critical concentration, $c = c_S$, where they start forming continuous geometries. Phase P grows fully continuous between $c = c_S$ and the second critical concentration, $c = c_P > c_S$, such that the composi-

te geometry from the latter concentration has become a mixture of discrete, de-agglomerating, phase S particles in a continuous phase P.

In other words: At concentration c_S, porous materials (P-pores) become very stiff when impregnated with a very stiff material. At the other critical concentration, $c = c_P > c_S$, the composite phase S elements become completely wrapped in a matrix of phase P. Porous materials loose their stiffness and strength at c_P because phase P has become a continuous, enveloping, void system.

In a complementary way the geometry history of phase S follows the history of phase P and vice versa. So-called shape functions (μ_P,μ_S) quantify the geometrical changes between c = 0 and c = 1. Shape factors (μ_P^o,μ_S^o) and (μ_P^1,μ_S^1) denote shape function values at c = 0 and at c = 1 respectively.

At fixed concentrations the following terminology is attached to the various stages of geometry changes just explained: DC means a discrete phase P in a continuous phase S. MM means a mixed phase P geometry in a mixed phase S geometry, while CD means a continuous phase P mixed with a discrete phase S.

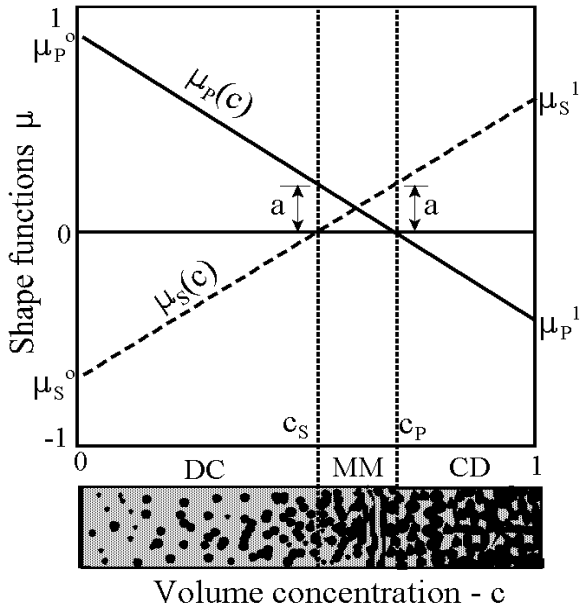

Figure 4. *Geometrical significance of shape functions: (μ_P,μ_S) = (+,-) means a discrete phase P in a continuous phase S. (μ_P,μ_S) = (+,+) means that both phases P and S appear with a mixed geometry. (μ_P,μ_S) = (-,+) means a continuous phase P mixed with discrete phase S elements. Black and gray signatures denote phase P and phase S respectively. (μ_P^o, μ_S^o,μ_P^1,μ_S^1) are so-called shape factors, (c_P, c_S) are so-called critical concentrations.*
The so-called geo-path factor, a, is explained in subsequent Section 2.1.2.

Formally the geometries explained above can be shifted along the concentration axis, c. A composite may develop from having a DC geometry at c = 0 to having a MM geometry at c = 1. Such composite geometries, with $c_P > 1$ and $0 < c_S < 1$, are named DC-MM geometries. Other composites may keep their DC type of geometry all the way up to c = 1 in which case the composite geometry is denoted as a DC-DC geometry, with both critical concentrations > 1. The specific geometry outlined in Figure 1 changes from DC to CD geometry which makes it a DC-CD geometry with both critical concentrations in c = 0-1.

A composite may develop from having a MM geometry at c = 0 to having a CD geometry at c = 1. Such composite geometries, with $0 < c_P < 1$ and $c_S < 0$, are named MM-CD geometries. Other composites may keep their MM type of geometry all the way up to c = 1 in which case the composite geometry is denoted a MM-MM geometry, with $c_P > 1$ and $c_S < 0$.

Ideal geometries at c = 0 and at c = 1 of a DC-CD composite are illustrated in Figures 2 and 3 respectively. We notice in this context that the composite theory deve-

loped in (1,2) is based on the concept that any isotropic composite geometry is a station on a geo-path moving *from the CSA_P geometry shown in Figure 2 to the CSA_S geometry shown in Figure 3.* (CSA is an abbreviation for the composite model, Composite Spheres Assemblage, introduced by Hashin in (3)).

Remarks: We notice that critical concentrations can be fictitious (outside c = 0 - 1). In such cases they do not, of course, have the immediate physical meanings previously explained. Formally, however, we do keep this 'explanation' in order to describe in an easy way, how the rate of changing the composite geometry is influenced by the processing technique used.

2.1.1 Classification of composites

For this paper the description of composite geometries are summarized in Table 1. For practice we introduce the following short sub-division of composites:

Particulate composites are defined by the former three rows in Table 1. They have particles in a continuous matrix geometry (DC) at small concentrations.

Lamella composites are defined by the latter two rows. They have mixed phase P geometry in a mixed phase S geometry (MM) at low concentrations.

Percolation

We notice that MM-geometries (if porous) are partly impregnable. This means that phase P percolation exists in composites with $c > c_S$. Percolation is complete for $c \geq c_P$. Porous materials have lost any coherence in this concentration area with no stiffness and strength left. (Percolation is connectivity of a phase across a microstructure. There is no percolation in a discrete phase – and full percolation in a continuous phase).

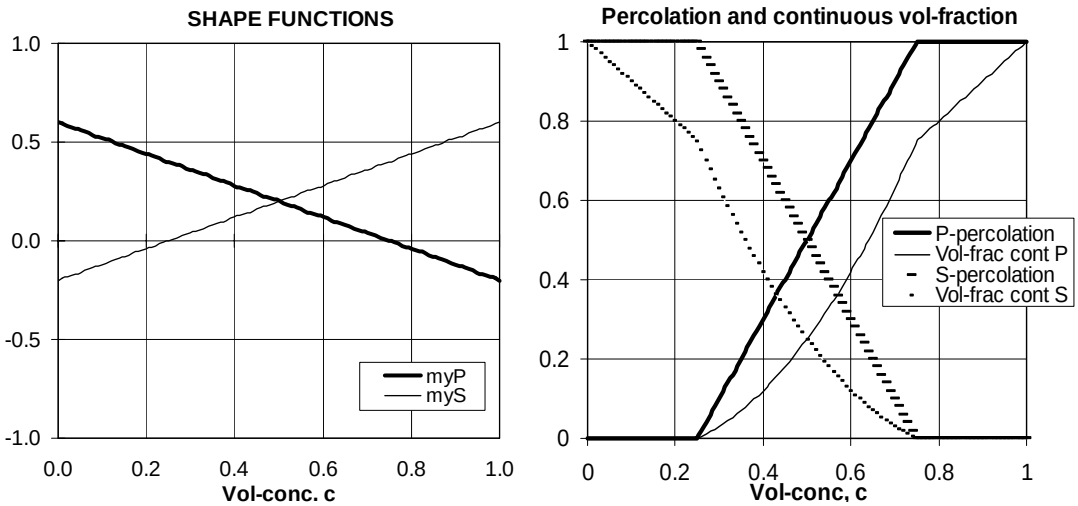

Figure 5. *Associated shape functions and graphs of percolation and continuous vol-fractions in phase P and phase S.*

Obviously, the phenomenon of percolation develops between the two critical concentrations. In Table 2 gray shadings indicate phase P percolation. We assume that percolation varies linearly from being 0 at $c \leq c_S$ to being 100% at $c > c_P$. Numerically, percolation is defined as γ = fraction of a phase being continuous. It can be expressed by Equation 7, where the so-called geo-path factor, a, is explained in the subsequent Section 2.1.2. A graphical representation of Equation 7 is presented in Figure 5.

$$\text{Percolation: } \gamma_P = \begin{cases} 0 & (c<c_S) \\ \frac{a-\mu_P}{a} & (c_S<c<c_P) \\ 1 & (c>c_P) \end{cases} \qquad \gamma_S = \begin{cases} 0 & (c>c_P) \\ \frac{a-\mu_S}{a} & (c_S<c<c_P) \\ 1 & (c<c_S) \end{cases} \qquad (7)$$

$$\text{Continuous volume fractions: } c_P^{CON} = c * \gamma_P \qquad c_S^{CON} = (1-c) * \gamma_S$$

PARTICULATE COMPOSITE $1 > \mu_P^o > -\mu_S^o > 0$				**EXAMPLES**
DC	**DC**	$c_S > 1$	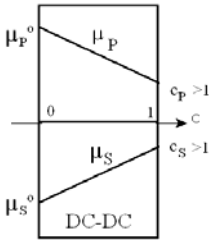	Particulate composite (concrete, mortar). Extremely high quality of grading (approaching CSA_P composites). *Pore system:* Not impregnable. Finite stiffness at any porosity
	MM	$1 > c_S > -\frac{\mu_S^o}{\mu_P^o}$	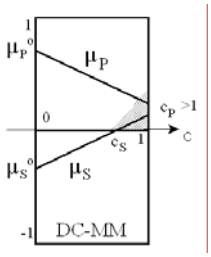	Particulate composite (concrete, mortar) with particle interference at $c = c_S$. Increasing quality of grading is quantified by larger concentration c_S at first interference. *Pore system:* Only impregnable for porosities $c > c_S$. Finite stiffness at any porosity.
	CD	$-\frac{\mu_S^o}{\mu_P^o} > c_S > -\frac{\mu_S^o}{1-\mu_S^o}$	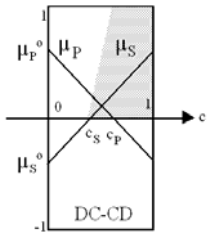	Mixed powders (ceramics). *Pore system:* Only impregnable for porosities $c > c_S$. No stiffness for porosities $c > c_P$.
LAMELLA COMPOSITE $1 > \mu_P^o > \mu_S^o > 0$				**EXAMPLES**
MM	**MM**	$c_S < -\frac{\mu_S^o}{\mu_P^o}$	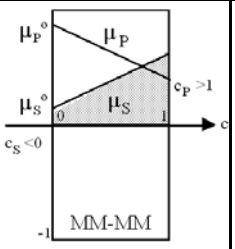	Mixed lamella/foils ("3D-plywood"). *Pore system:* Fully open at any porosity. Finite stiffness at any porosity.
	CD	$-\frac{\mu_S^o}{\mu_P^o} < c_S < -\frac{\mu_S^o}{1-\mu_S^o}$	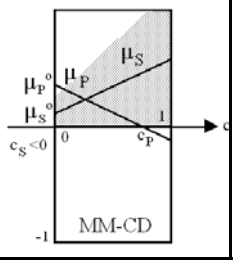	Mixed lamella/foils ("3D-plywood"). *Pore system:* Fully open at any porosity. No stiffness for porosities $c > c_P$.

Table 1. *Classification of composite materials. μ_P^o,μ_S^o are shape factors. c_S is the first critical concentration. The second critical concentration, c_P, is deduced by $c_P = -c_S * \mu_P^o / \mu_P^o$. Shaded areas denote percolation in phase P.*

2.1.2 Shape functions

Shape functions quantify the specific types of geometries considered (e.g. DC-CD, DC-MM, and others). After some re-writing of an expression presented in (1) the two shape functions can be expressed approximately by Equation 8[2)] where the three input parameters are explained in Equation 9 – and further considered in subsequent sections. Notice that the two shape functions are related by the so-called geo-path factor $a = \mu_P + \mu_S$.

$$\begin{aligned}&\text{Given: } a,\ \mu_P^o,\ \text{and } c_S\\ &\text{Calculate: } \mu_S^o = a - \mu_P^o \ \text{ and } \ c_P = \frac{c_S}{1 - a/\mu_P^o}\\ &\text{Then shape functions are: } \mu_P = \mu_P^o\left(1 - \frac{c}{c_P}\right) \ ; \quad \mu_S = \mu_S^o\left(1 - \frac{c}{c_S}\right)\\ &\text{Then truncate shape functions to hold } -1 \le \mu_P, \mu_S \le 1\end{aligned} \tag{8}$$

$0 \le a \le 1$ is geo-path factor (increasing with length of phase components)

$\mu_P^o > a$ for particulate composites
$\mu_P^o < a$ for lamella composites
is shape factor (estimate from Figure 6) (9)

c_S is first critical concentration (estimate from Table 1)

Remark: Expression 8 is a simplification of more complete shape functions described in (1) where the critical concentration c_P and the shape factor μ_S^o are independent geometrical quantities – and where the shape functions are related in a more general way then expressed by a simple geo-path factor. However, the simple shape function description has been justified in (1) to act as a good approximation in a number of composite analyses.

Particulate composite (DC-DC, DC-MM, DC-CD)
Uni-shape particles
$\mu_P^o = \frac{3A}{A^2 + A + 1}$ for $A \le 1$; $\mu_P^o = 3\frac{A^2 - A + 1}{4A^2 - 5A + 4}$ for $A > 1$
Multi-shape particles [3)]
$\mu_P^o \simeq \left(\sum_{i=1}^{\infty} \frac{\alpha_i}{\mu_{P,i}^o}\right)^{-1}$; α_i is volume fraction of A_i $\mu_{P,i}^o$ is shape factor individually determined for A_i from section 'uni-shape particles'
Lamella composites (MM-MM, MM-CD)
$\mu_P^o \approx a(1 - \gamma)$ with basic shapes agglomerating, a = geo–path factor $\approx$ 0.75-1 long fibres; 0.5 fibres+ discs; 0 discs Percolation, $\gamma \approx 0 - 1$

Table 2*. Shape factors for various phase geometries at c = 0.*

2) The truncation procedure in Equation 8 causes CSA geometries close to c = 0 and c = 1 to be described correctly by, formally, introducing $\mu_P^o > 1$.

3) This is an approximation of a more accurate (and complicated) expression presented in (1).

Shape factors

Shape factors can be estimated from Table 2 and/or Figure 6 developed on the basis of an analysis of dilute particulate composites and a FEM analysis of MM-MM composites in (1).

For a particulate composite with particles of the same shapes, shape factors can be determined from the former section ('uni-shape particles') of Table 2. The so-called aspect ratio, A = length/diameter of particles. Spherical particles have A = 1. Long particles have A > 1. Flat (short) particles have A < 1.

For particulate composites with a distribution of particle shapes ('multi-shape particles'), shape factors can be calculated by the second section of Table 2. For lamella composites shape factors are calculated from the latter section.

Remark: To be consistent with our intentions stated in Section 1.1 to keep geometrical descriptions simple, we will, subsequently, use Table 2 mainly to frame correct orders of magnitudes for shape factors. In general, shape factors will be estimated directly from Figure 6 respecting the magnitudes (a) of geo-path factors as they are presented in Equation 9.

Geo-path and quantification of processing

The geo-path graph shown in Figure 6 is a convenient way of describing the type of geometries traversed when the volume concentration of phase P proceeds from c = 0 (start of path) to c = 1 (end of path). The geo-path is easily constructed from the shape functions. The details of Figure 6 are determined from information presented in (1).

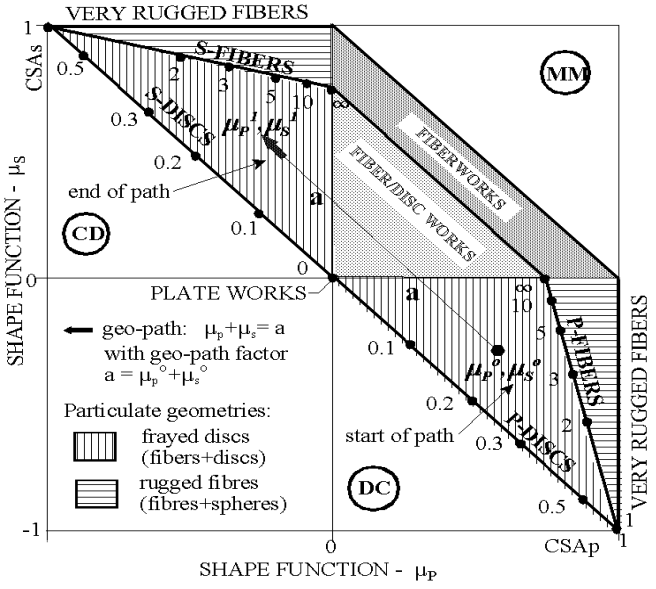

Figure 6. *<u>Geo-path graph</u>: $\mu_P + \mu_S = a$*

Numbers in section DC indicate aspect ratios A = length/diameter of phase P-particles. Correspondingly, numbers in section CD indicate aspect ratios of S-particles.
<u>Particulate composites</u>:
Vertical lines: Frayed discs: Mixture of discs and fibers ('jelly fish')
Horizontal lines: Rugged fibers: Mixture of fibers and spheres ('shark eggs')
<u>Lamella composites</u>:
Light gray: Agglomerating frayed discs with degree of agglomeration = percolation.
Dark gray: Agglomerating rugged fibers with degree of agglomeration = percolation.

We notice that geo-paths orientated according to Figure 6 means that the shape function μ_P decreases with c while μ_S increases with c. Such behavior agrees with the basic concept of geometry changes previously introduced: Every phase geometry considered is a station on a continuously change of going from a CSA_P geometry to a CSA_S geometry.

The geo-path factor, a, is a significant parameter in the shape function description. With some confidence we suggest, as a hypothesis, that the geo-path factor can be used to quantify different processing techniques.

Critical concentration

Critical concentrations depend very much on the processing technique used to produce composites. As we do not, to day, know very much about the influence of processing on phase geometry we have to trust estimates based on experience, experiments, and general observations as the ones previously mentioned: At concentration c_S, porous materials (P-pores) become very stiff when impregnated with a very stiff material. c_S can also be thought of as the concentration at first interference of phase P (starting to create a continuous skeleton). At the other critical concentration, $c = c_P > c_S$, the composite phase S elements become completely wrapped in a matrix of phase P. Porous materials loose their stiffness and strength at c_P because phase P has become a continuous, enveloping, void system.

3. PREDICTION OF COMPOSITE PROPERTIES

As previously mentioned, the global composite property solutions presented in Section 1.2 can be converted to solutions for composites with specific phase geometries only by introducing the associated shape functions, μ into the geo-function, θ. The conversion is made as explained in Equation 10.

$$\text{Geo - function for stiffness analysis :}$$
$$\theta = \frac{1}{2}\left[\mu_P + n\mu_S + \sqrt{(\mu_P + n\mu_S)^2 + 4n(1 - \mu_P - \mu_S)} \right] \; ; \; n = \frac{E_P}{E_S}$$
$$\text{Geo - function for conductivity analysis :} \qquad (10)$$
$$\theta_Q = \mu_P + nQ\mu_S + \sqrt{(\mu_P + nQ\mu_S)^2 + 4nQ(1 - \mu_P - \mu_S)} \; ; \; nQ = \frac{Q_P}{Q_S}$$

4. MATERIALS DESIGN

The statement that composite properties depend very much on composite geometry has been justified/demonstrated in a number of examples, presented in (1). A very satisfying agreement between theoretical predictions and experimentally obtained data are observed. Some examples considered are: Particles mixed into a continuous matrix, compaction of powders, production of porous materials, impregnation of porous materials, particulate composites with self-inflicted pores (light clinker concrete), and three-dimensional 'Plywood' composites, thermal eigenstrain, self-compacting concrete, and viscoelastic composites.

It then seems justified to state that the quality of the present theory to work with global descriptions (θ) of composite geometries qualifies it to be used in design of composite materials, meaning that the theory has the potential of predicting composite geometries which will 'produce' prescribed composite properties.

We will explore this statement performing an inverse analysis of the composite expressions previously presented. Keeping our source materials, Phase P and Phase S, such analysis can be made with the following results applying for the simple geo-path description, $\mu_P + \mu_S = a$, previously introduced.

4.1 Geometry versus composite property

With a prescribed Young's modulus of E, or conductivity Q, at volume concentration c the shape function values are determined by Equations 11 derived from Equations 1, 5, and 10.

With two prescribed Young's moduli, or two conductivities two accurate shape function values can be determined. Then, full shape functions (μ_P,μ_S) can be extrapolated using that shape functions vary linearly with volume concentrations, see Figure 1.

Stiffness

$$\theta = \frac{[n - c(n-1)]e - n}{1 + c(n-1) - e} \quad \Rightarrow \quad \mu_S = \frac{n(1-a) + \theta(a-\theta)}{\theta(1-n)} \quad \text{and} \quad \mu_P = a - \mu_S$$

Conductivity

$$\theta_Q = \frac{[n_Q - c(n_Q - 1)]q - n_Q}{1 + c(n_Q - 1) - q} \Rightarrow \mu_S = \frac{4n_Q(1-a) + \theta_Q(2a - \theta_Q)}{2\theta_Q(1 - n_Q)} \quad \text{and} \quad \mu_P = a - \mu_S \qquad (11)$$

Remark: The better extrapolated shape function values are always those between the accurate ones deduced directly with Equation 11. Extrapolated shape functions (as just described), may become greater than 1 or less than –1 at low and high volume concentrations. This means that CSA geometries are approached at these concentrations. In such cases, the shape functions must be truncated to hold $-1 \le \mu \le 1$ before using them for prediction purposes (see Equation 8). This feature is demonstrated in the following example in Section 5.1.2, which also indicates that a number of possible composite geometries are revealed by varying the geo-path factor (processing).

Important note: It is emphasized that prescribed quantities, of coarse, ***must not violate the property bounds*** presented in Equation 6.

5. EXAMPLES

5.1 Composite with prescribed chloride diffusivity

We know from experiments the conductivity of a two-phase composite at two volume concentrations. We would like to know the conductivity of the composite at any concentration. (The specific conductivity considered is chloride diffusivity of saturated cement paste).

In order to solve this problem we must apply both 1) the design procedure (Section 4) and 2) the prediction procedure (Section 3) explained in this paper.

Source materials: Phase S and Phase P have $(Q_P,Q_S)/Q_P = (1,0.00008)$ with $Q_P = 2*10^{-9}$ m^2/sec.

Prescribed composite conductivities: $(Q_1,Q_2)/Q_P = (0.0013,0.1072)$ at $(c_1,c_2) = (0.215, 0.397)$. These conductivities have been chosen from chloride diffusion experiments on saturated cement paste reported in (9,10) (6% Si).

This choice has been made in order to justify the analysis by comparing the results obtained with a number of other experimental data presented in (9,10).

5.1.1 Results

A fine result of a design analysis is obtained with a = 0.4 for which the composite geometry shown in Figure 7 is revealed with $(\mu_P^o, c_S) = (0.576, 0.243) \Rightarrow (\mu_S^o, c_P) = (-0.176, 0.798)$.

These parameters correspond to a DC-CD composite based on pores of medium length (a mixture of $A \approx 0.2$ and $A \approx 10$, see Figure 6).

Predicted conductivity (by Equation 5) of a composite with this geometry is shown in Figure 8. Also shown in this figure are further experimental data from (9,10). The excellent agreement between predicted and all experimental data proves very much the reliability of both the design analysis and the prediction analysis presented in this example.

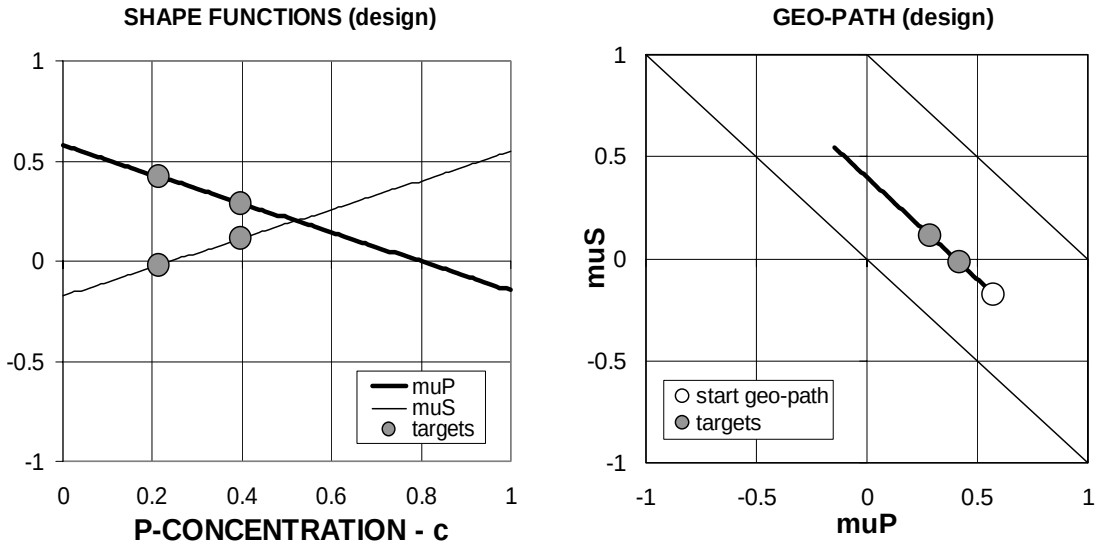

Figure 7. *Geometry of a composite with prescribed chloride diffusitivity $(Q_1,Q_2)/Q_P$ = (0.0013,0.1072) respectively at (c_1,c_2) = (0.215,0.397). A geo-path factor of a = 0.40 is used.*

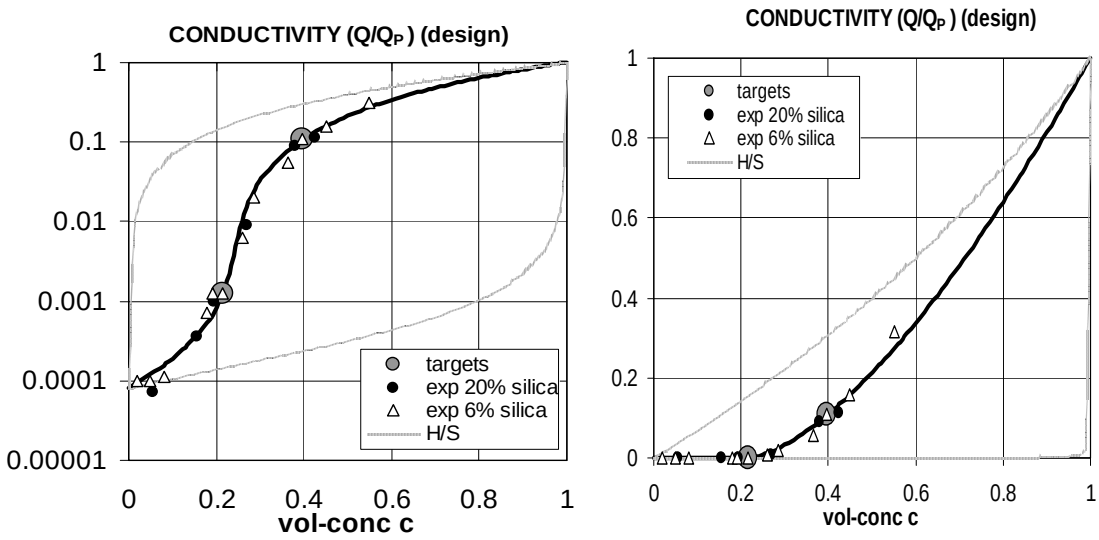

Figure 8. *Conductivity in composite designed from prescribed chloride diffusitivity of composite with geometry defined in Figure 7 (a = 0.4).*

5.1.2 Alternative geometries

We will now look at the same design example as just considered. The only difference is that the design analysis is now made with another geo-path factor, namely a = 0 and a = 1. The purpose of this analysis is 1) to illustrate the statement previously made, that various composite geometries may approximately 'produce' similar composite properties – and 2) to illustrate the consequence of deduced shape functions to violate $|\mu| \leq 1$.

Geo-path factor a = 0 (disc pores)

The composite geometry deduced is presented in Figure 9. The conductivities predicted by Equation 5 and this geometry are shown in Figure 10. It is noticed that the prescribed conductivities, of course, are described accurately. The overall prediction of conductivities, however, is almost as good as presented in Figure 8 with a = 0.4.

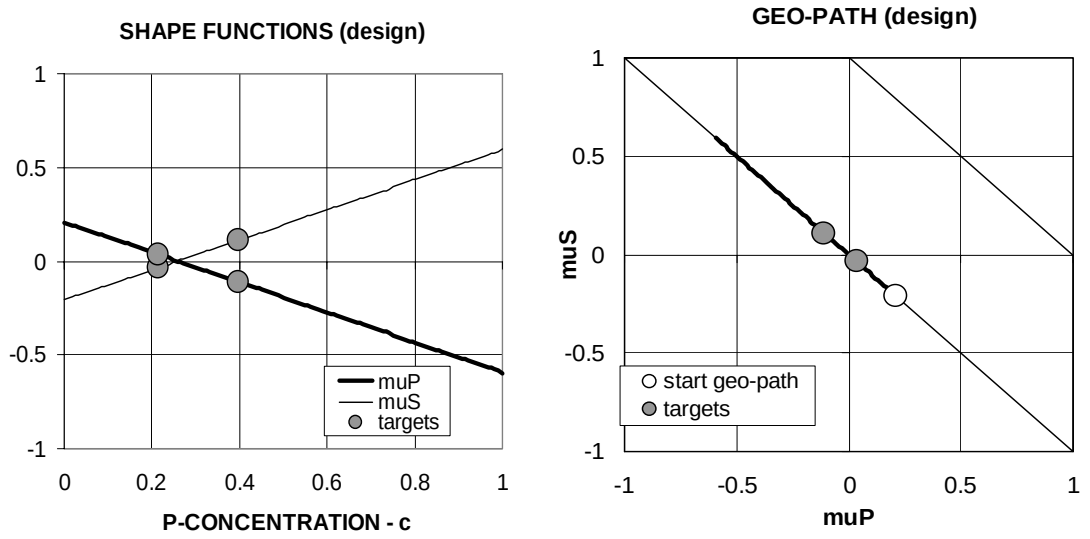

Figure 9. *Geometry of a composite with prescribed chloride diffusitivity $(Q_1,Q_2)/Q_P$ = (0.0013,0.1072) respectively at (c_1,c_2) = (0.215,0.397). A geo-path factor of a = 0 is used.*

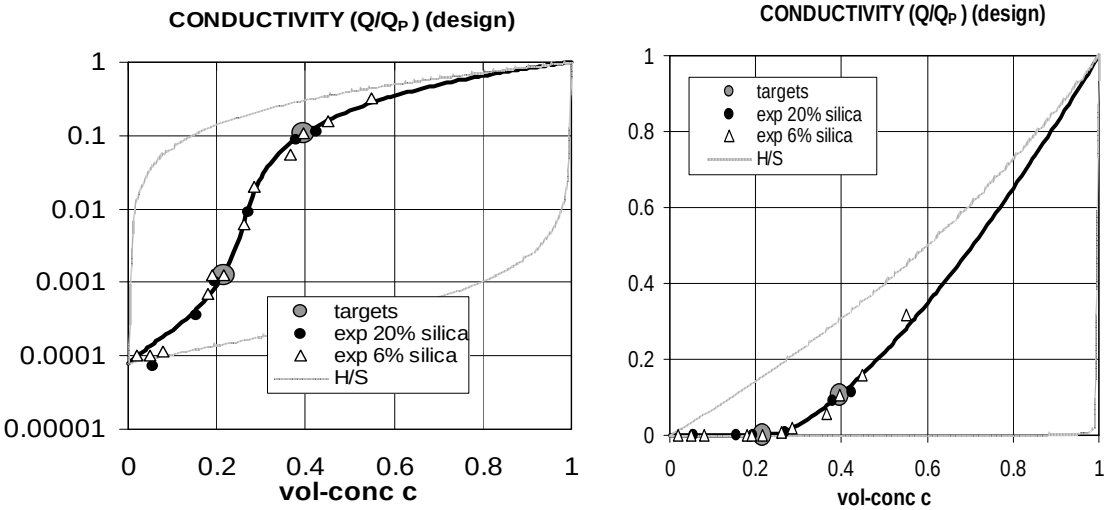

Figure 10. *Conductivity in composite designed from prescribed chloride diffusitivity of composite defined in Figure 9 (a = 0).*

Geo-path factor a = 1 (long pores)

The composite geometry deduced is presented in Figure 11 with a truncation introduced on the phase P shape function (see Section 4.1). The conductivities predicted by Equation 5 and this geometry are shown in Figure 12. It is noticed that the prescribed conductivities, of course, are described accurately. At low porosities, predicted conductivity is influenced by the shape function truncation introduced such that lower bound (CSA-geometry) solutions are predicted.

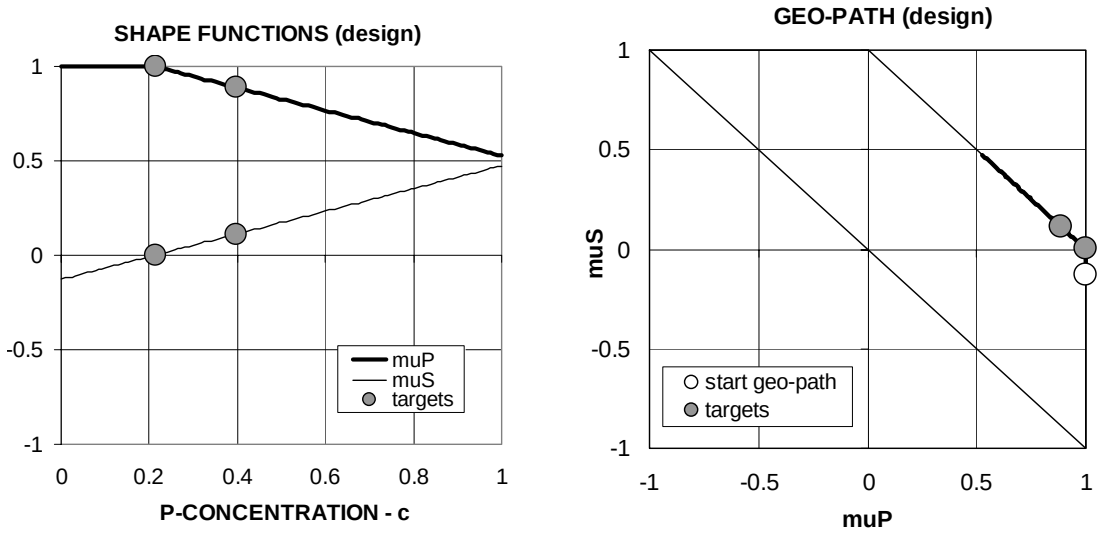

Figure 11. *Geometry of a composite with prescribed chloride diffusitivity $(Q_1,Q_2)/Q_P$ = (0.0013,0.1072) respectively at (c_1,c_2) = (0.215,0.397). A geo-path factor of a = 1 is used.*

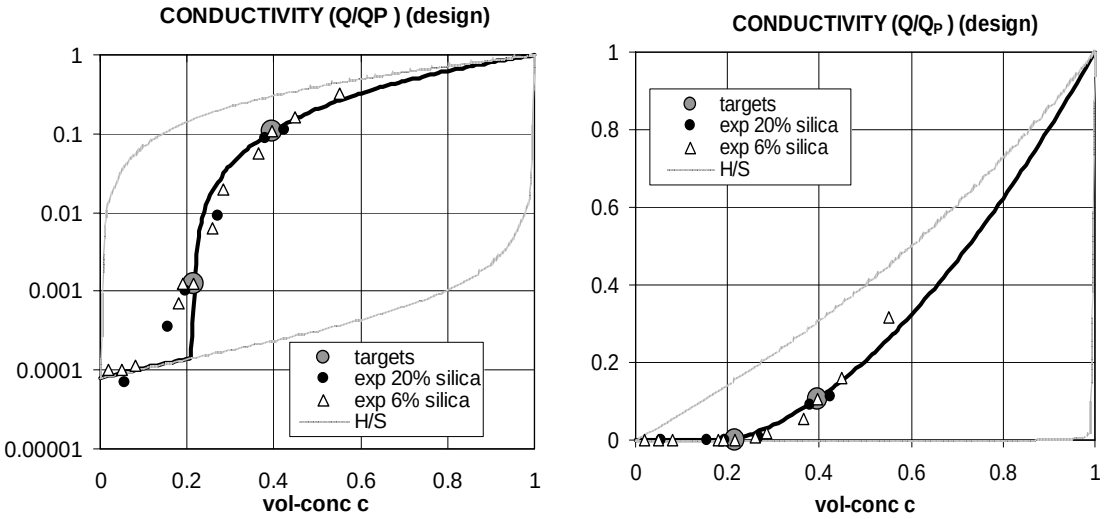

Figure 12. *Conductivity in composite designed from prescribed chloride diffusitivity of composite with geometry defined in Figure 11 (a = 1).*

5.2 Porous material with prescribed stiffness

We know from experiments the stiffness at two porosities of a porous material (HCP). We would like to know the composite geometry such that stiffness can be determined at any porosity.

In order to solve this problem we must apply both 1) the design procedure (Section 4) and 2) the prediction procedure (Section 3) explained in this paper.

Sources: The components are phases (P,S) = (capillary pores, cement gel). The following phase properties are deduced from information reported in (11,12): The stiffness of bulk cement gel and pores are E_S = 36000 MPa and E_P = 0 MPa respectively.

Prescribed composite stiffness: (E_1,E_2) = (17200,8210) MPa at (c_1,c_2) = (0.22,0.42). These data have been chosen from stiffness experiments on the cement paste reported in (11,12). This choice has been made in order to justify the analysis by comparing the results obtained with a number of other experimental data presented (11,12).

5.2.1 Results

A fine result of a design analysis is obtained with a = 0.4 for which the composite geometry shown in Figure 13 is revealed with (μ_P^o, c_S) = (0.431,0.082) $\Rightarrow$ (μ_S^o, c_P) = (-0.03,1.14). These parameters correspond to a DC-MM composite based on pores of medium length (a mixture of A $\approx$ 0.1 and A $\approx$ 25, see Figure 6).

Predicted stiffness of a composite with this geometry is shown in Figure 14. Also shown in this figure are further experimental data from (11,12). The excellent agreement between predicted and all experimental data proves very much the reliability of both the design and the prediction analysis presented in this example.

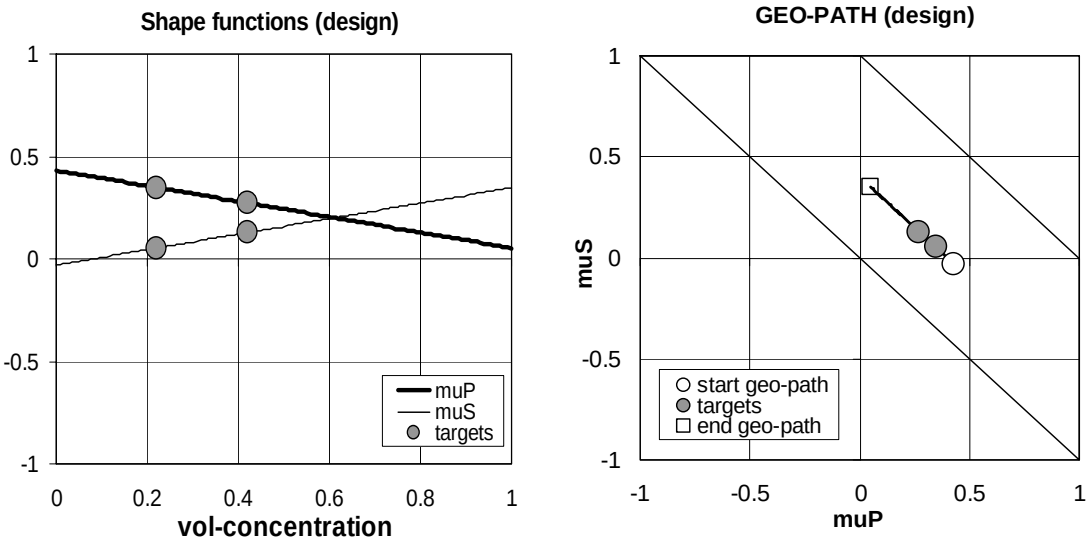

Figure 13. *Geometry of empty cement paste considered.*

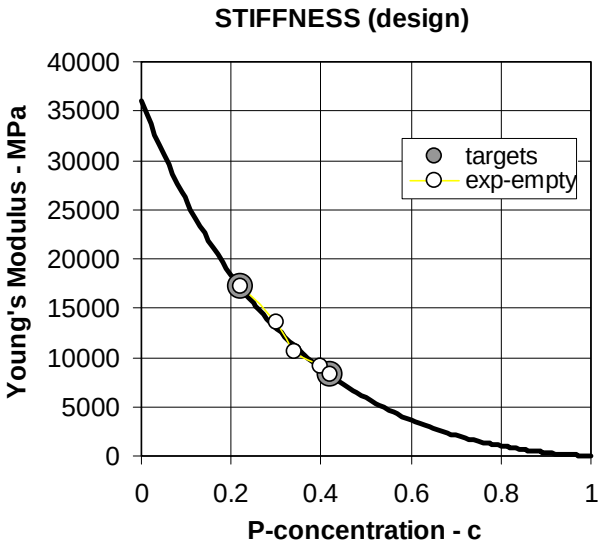

Figure 14. *Empty cement paste system considered: Stiffness as related to capillary porosity*

5.3 Stiffness of impregnated porous material

The cement paste just considered is impregnated with Sulphur the stiffness of which is E_P = 11000 MPa (modified with respect to an impregnation degree of 82%). Which stiffness can be expected for this material?

The shape functions (Figure 13) previously determined for the empty cement paste quantify the composite geometry. Thus, the problem to solve is a plain prediction problem. Equation 1 can immediately be used to determine the stiffness in question. The result is shown in Figure 15 together with experimental data presented in (12).

The excellent agreement observed verifies that shape functions are independent of phase properties.

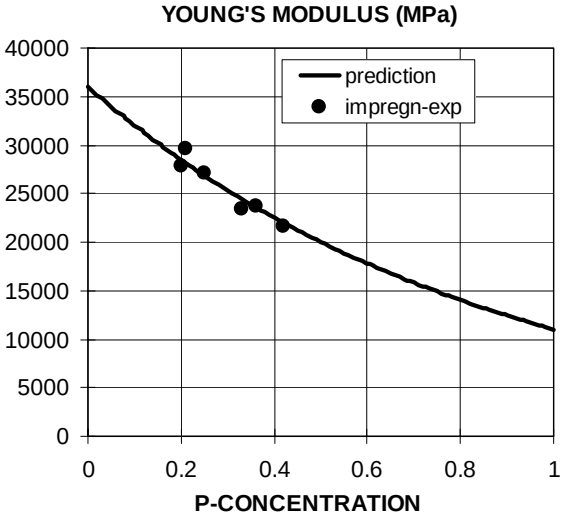

Figure 15. *Stiffness of Sulphur impregnated cement paste (the same as considered in previous example).*

Remark: It is interesting to notice that the geometry, Figure 7, of the cement paste considered in Section 5.1.1 is very familiar with the one, Figure 13, deduced for the cement paste in the present example. Apparently the cement pastes used in all (9,10, 11,12) have geometries, which are similar, and produced with the same technology (a = 0.4).

6. CONCLUSIONS AND FINAL REMARKS

A theory has been presented in this paper, by which properties can be predicted for composites with various phase geometries.

The theory is inversed to predict which type of phase geometries will create prescribed material properties.

Both versions of the theory are applied successfully on examples of practical relevance, such as: 1) Chloride diffusivity of HCP and 2) Stiffness prediction of empty and impregnated HCP (hardened cement paste).

Remark: Deliberately, the theory presented is based on simple descriptions of geometry variations, including a simple quantification of fabrication techniques. There are two reasons for that: We should not exaggerate our present knowledge, 1) on general descriptions of composite geometries – and 2) on quantification of specific technologies, which, in practice, can produce prescribed geometries.

In order to improve/modify the methods presented in this paper the two topics, 1) and 2), have to be considered in a joint research effort involving both theoretical (including FEM such as in (1)) and technological means.

Notations

We notice that the notation used in this paper is similar to the one used in (1). The list does not consider less general symbols, which are explained locally. Notations used by the author prior to his work in (1) are somewhat different.

Abbreviations and subscripts	
V	Volume
P	Phase P
S	Phase S
No subscript	Composite materials
H/S	Hashin/Shtrikman's property bounds
Geo-parameters	
$c = V_P/(V_P+V_S)$	Volume concentration of phase P
μ^o,μ^1	Shape factors
μ_P	Shape function
μ_S	Shape function
a	Geo-path factor
c_P,c_S	Critical concentrations
γ	Percolation
θ	Geo-function for stiffness
θ_Q	Geo-function for conductivity
Stiffness and other properties	
E	Stiffness (Young's modulus)
$e = E/E_S$	Relative stiffness of composite
$n = E_P/E_S$	Stiffness ratio
Q	Conductivity (e.g. thermal, electrical, diffusivity)
$q = Q/Q_S$	Relative conductivity of composite
$n_Q = Q_P/Q_S$	Conductivity ratio
Stress and strain	
σ	External mechanical stress
σ_P	Phase P stress caused by external mechanical stress
σ_S	Phase S stress caused by external mechanical stress
λ	Linear eigenstrain (e.g. shrinkage, thermal expansion)
$\Delta\lambda = \lambda_P-\lambda_S$	Linear differential eigenstrain
ρ	Hydrostatic stress caused by eigenstrain

Literature

1. Nielsen, L. Fuglsang: "Composite Materials – Properties as influenced by phase geometry", Springer Verlag, Berlin, Heidelberg 2005.

2. Idem: "Elastic Properties of Two-Phase Materials", Materials Science and Engineering, 52(1982), 39-62.

3. Hashin, Z.: "Elastic moduli of heterogeneous materials". J. Appl. Mech., 29 (1962), 143 - 150.

4. Budiansky, B.: On the elastic moduli of some heterogeneous materials". J. Mech. Phys. Solids, 13(1965), 223 - 227.

5. Böttcher, C.J.F.: "The dielectric constant of crystalline powders", Rec. Trav. Pays-Bas, 64(1945), 47.

6. Maxwell, J.C.: Treatise on electricity and magnetism, 1(1873), 365.

7. Hashin, Z. and Shtrikman, S.: "Variational approach to the theory of elastic behavior of multi-phase materials". J. Mech. Solids, 11(1963), 127 - 140.

8. Idem: "A variational approach to the theory of the effective magnetic permeability of multi-phase materials", J. Appl. Phys. 33(1962), 3125.

9. Bentz, D.P., O.M. Jensen, A.M. Coats, and F.P. Glasser: "Influence of silica fume on diffusivity in cement-based materials. Part I: Experimental and computer modeling studies on cement pastes", Cement and Concrete Research, 30(2000), 953-962.

10. Jensen, O.M.: "Chloride ingress in cement paste and mortar measured by Electron Probe Micro Analysis", Report R51(1998), Department of Structural Engineering and Materials, Technical University of Denmark.

11. Beaudoin, J.J. and R.F. Feldman: "A study of mechanical properties of autoclaved Calcium silicate systems", Cem. Concr. Res., 5(1975), 103-118.

12. Feldman, R.F. and J.J. Beaudoin: “Studies of composites made by impregnation of porous bodies. I: Sulphur impregnant in Portland cement systems", Cem. Concr. Res., 7(1977), 19-30.